Simulation of cavitation bubbles in travelling acoustic waves

Philipp Koch, Robert Mettin and Werner Lauterborn
Drittes Physikalisches Institut, Universität Göttingen, Bürgerstr. 42-44, 37073 Göttingen, Germany

Introduction

Acoustic cavitation near ultrasonic emitters of the sonotrode type can form certain structures of fast moving bubbles [1]. We investigate if the special pressure field geometry can give a reason for such formations. In a particle model, we assume a damped travelling wave moving away from the transducer surface. The continuous phase variation yields to a second part of the primary Bjerknes force, which can partly explain the bubble behavior.

Particle modelling

Our simulation considers each bubble as one single entity [2]. The following forces on every bubble are added up, and the equations of motion are solved by numerical integration:

$$\begin{aligned}
\vec{F}^i_{\mathrm{M}} &= \frac{\varrho}{2}\left\langle V^i\right\rangle_\tau \ddot{\vec{x}}^i \\
\vec{F}^i_{\mathrm{D}} &= -\alpha\dot{\vec{x}}^i, \quad \alpha = 12\pi\mu\left\langle R^i\right\rangle_\tau \\
\vec{F}^i_{\mathrm{Bp}} &= -\left\langle \nabla p_{\mathrm{S}} \cdot V^i\right\rangle_\tau \\
\vec{F}^i_{\mathrm{Bs}} &= \frac{\varrho}{4\pi}\sum_{j\neq i}\left\langle \dot{V}^i(t)\cdot\dot{V}^j(t)\right\rangle_\tau \cdot \frac{\vec{d}^{\,i,j}}{|\vec{d}^{\,i,j}|^3}
\end{aligned}$$

Here i is the bubble index, $\vec{x}$ the bubble position, V the bubble volume, μ the viscosity, ϱ the liquid density and $d^{i,j} = \vec{x}^j - \vec{x}^i$ the distance between bubble i and j. The primary Bjerknes force $\vec{F}_{\mathrm{Bp}}$ describes the effect of the external pressure field onto the bubble translation. Interaction of two bubbles are accounted for by the secondary Bjerknes force $\vec{F}_{\mathrm{Bs}}$. $\vec{F}_{\mathrm{M}}$ is the virtual mass (inertia) force and $\vec{F}_{\mathrm{D}}$ the viscous drag force. By averaging over the sound field period τ the translation and oscillation of the bubbles become uncoupled.

The pressure at the bubble position, p_{S}, is given from a pressure field for a single driving frequency $\omega = 2\pi\nu = \frac{2\pi}{\tau}$ and spatially varying amplitude p_{A} and phase φ:

$$p_{\mathrm{S}} = p_{\mathrm{A}} \cdot \cos(\omega t - \varphi)$$

With this pressure the primary Bjerknes force can be split into two parts:

$$\begin{aligned}
\vec{F}_{\mathrm{Bp}} &= -\nabla p_{\mathrm{A}} \cdot \langle\cos(\omega t)\cdot V\rangle_\tau \\
&\quad -\nabla\varphi \cdot p_{\mathrm{A}} \cdot \langle\sin(\omega t)\cdot V\rangle_\tau \qquad (1)
\end{aligned}$$

The first term on the right hand side alone describes an ideal standing wave with constant phase and $\nabla\varphi = 0$, which is identical to previous formulations [3, 2, 4]. For constant pressure amplitude $\nabla p_{\mathrm{A}} = 0$ the first term vanishes and only the term with the phase gradient contributes, like in an ideal plane travelling wave [5].

Sonotrode

The setup geometry is shown in Fig. 1. The sonotrode of diameter $2a$ is dipped from top into a tank with water.

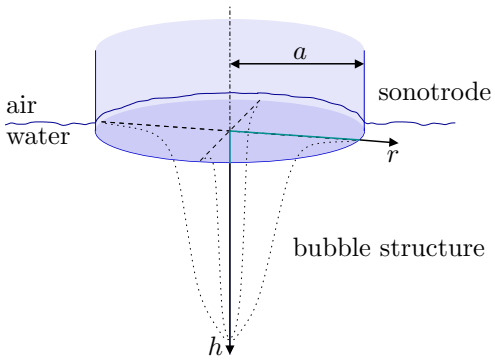

Figure 1: Schematic plot of the sonotrode geometry and coordinates.

The pressure field below the sonotrode is assumed as a travelling wave with a gaussian profile along the radius axis and a damping (due to cavitation).

$$\begin{aligned}
p_{\mathrm{S}} &= p_{\mathrm{A}} \cdot \exp(-r^2/A^2) \cdot \exp(-h\cdot B) \cdot \cos(\omega t - \varphi) \\
\varphi &= (2\pi/\lambda)\cdot h \qquad (2)
\end{aligned}$$

Fig. 2 shows the radially symmetric amplitude of this pressure field (wavelength $\lambda = 7.5$ cm; frequency $\nu = 20$ kHz).

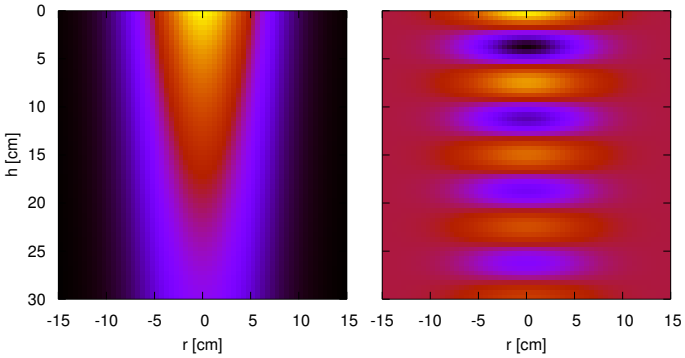

Figure 2: Pressure field below the sonotrode from (2) with $A = 6$ cm and $B = 400$ cm; left: pressure amplitude; right: pressure p_{A} at $t = 0$ s.

Along the radial axis the pressure field is formed without phase variation. The primary Bjerknes force acts in high pressure regimes repulsive near the symmetry axis and switches its sign in a distance depending on the pressure amplitude (equilibrium bubble radius $R_{\mathrm{n}} = 5$ μm).

Because of the damping of the travelling wave, the first term of (1) is also not zero in vertical direction ($\frac{\partial}{\partial h}p_{\mathrm{A}} \neq$

0). This yields to an attractive force on the bubbles towards the sonotrode ($R_n = 5$ μm). The second term in (1) for $\nabla\varphi \neq 0$ acts repulsive in the near field. By the sum of these two effects the bubbles are driven to the point on the symmetry axis at which they balance each other (Fig. 3).

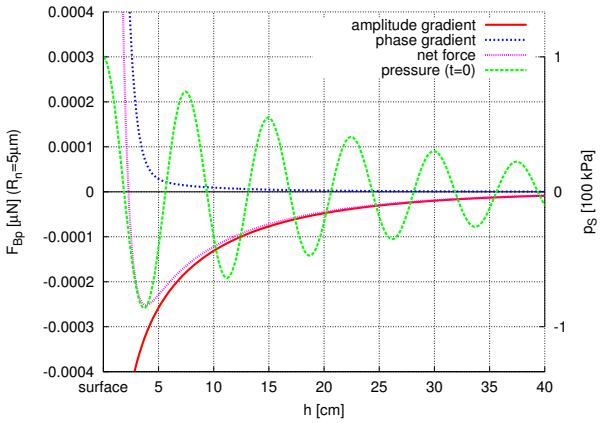

Figure 3: Superposition of the amplitude and phase gradient parts of the primary Bjerknes force along the symmetry axis ($p_A = 100$ kPa, $R_n = 7$ μm).

Results

The normalized primary Bjerknes force vectors are shown in Fig. 4. The arrows are pointing into the direction in which a bubble with $R_n = 5$ μm equilibrium radius will be forced at a pressure amplitude of $p_A = 300$ kPa. The highlighted area marks the region in which the bubble moves towards the symmetry axis and is pushed away from the sonotrode. It is the outer boundary of the formed bubble structure for these parameters.

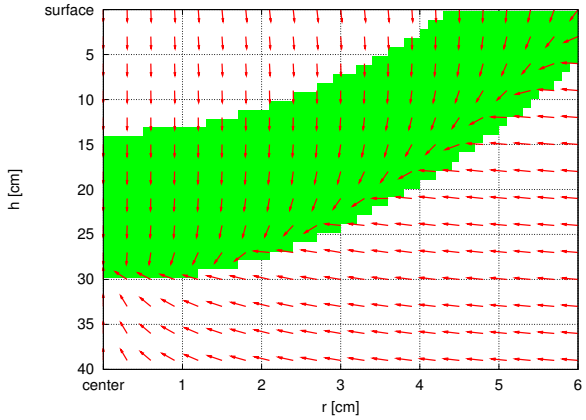

Figure 4: Arrows indicate the pointing of the primary Bjerknes force, the highlighted area indicates the possible structure shape ($p_A = 300$ kPa, $R_n = 5$ μm).

By our calculations the dimensions of the cone-like bubble structure depends on the pressure amplitude p_A and the bubble equilibrium radius R_n as well as on the pressure field geometry. The geometry is held fixed for all calculations shown (Fig. 2). We can demonstrate the transformation by varing p_A and R_n. Fig. 5 shows bubble formation around the symmetry axis ($r = 0$ cm). Bubbles are seeded at the sonotrode surface $h = 0$ cm and $r = 4 \ldots 6$ cm. In the left picture the bubbles are forming a smaller figure with a round tip. For higher pressure amplitudes this figure grows up and the tip becomes more spiky. In the same way bubbles were forced away from the sonotrode surface for larger values of r. In both calculations a typical curve at the separating area of the bubbles from the surface can be observed.

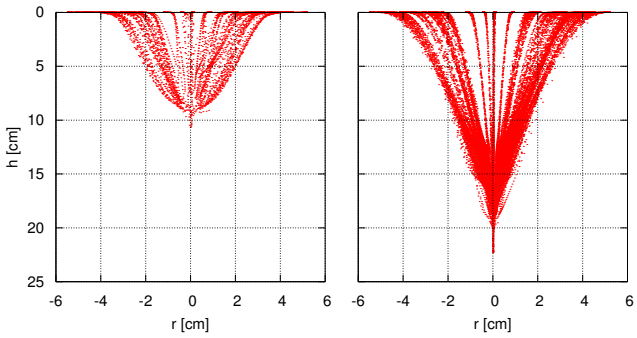

Figure 5: Cavitation bubble structure below the sonotrode (sonotrode surface at the top of the images); left: $p_A = 100$ kPa, $R_n = 7$ μm. right: $p_A = 150$ kPa, $R_n = 4$ μm.

The bubble velocities increase with growing pressure amplitude and for larger equilibrium radius. In the calculation for $p_A = 100$ kPa, $R_n = 7$ μm the velocity reach $v \approx 0.1$ m/s; in the $p_A = 150$ kPa, $R_n = 4$ μm case it is $v \approx 0.2$ m/s. Experimental oberservations of bubbles in cone structures yield velocities at $v \approx 1$ m/s.

Conclusion and outlook

The used pressure field geometry is an approximation that yields two acceptable results. Changes of the geometry affects on the shape of the bubble structures. Future work will be done for calculations of different experimentally observed bubble structures with special attention on the pressure field geometry.

Acknowledgement

This work was supported by the German Ministry of Education and Research (BMBF project "Untersuchung von Kavitationsfeldern"). P. K. acknowledges the generous support by the Deutsche Forschungsgemeinschaft (Graduiertenkolleg "Strömungsinstabilitäten und Turbulenz").

References

[1] A. Moussatov, R. Mettin, C. Granger, T. Tervo, B. Dubus and W. Lauterborn, Proceedings of the 2003 WCU, Paris, 955-958.

[2] R. Mettin, S. Luther, C.-D. Ohl and W. Lauterborn, Ultrasonics Sonochemistry 6, 25-29, 1999.

[3] T. G. Leighton, *The Acoustic Bubble*, Academic Press, 1994.

[4] W. Lauterborn, T. Kurz, R. Mettin, and C.-D. Ohl, in: I. Prigogine and S.A. Rice (eds.): Advances in Chemical Physics 110, pp. 295-380, John Wiley & Sons, New York (1999).

[5] K. Yosioka and Y. Kawasima, Acustica, vol. 5, 167-178, 1955.